ce/papers Proceedings in civil engineering

Ernst & Sohn A Wiley Brand

ORIGINAL ARTICLE

eurosteel AMSTERDAM 2023

Ernst & Sohn A Wiley Brand

Plate and stiffener buckling in transversely loaded steel panels

Svein-Rune Kleppe[1,2] | Arne Aalberg[2]

Correspondence

Assistant professor Svein-Rune Kleppe
Western Norway University of Applied Science, Department of Civil Engineering.
Inndalsveien 28, 5063 Bergen.
Email: srk@hvl.no

[1] Western Norway University of Applied Science, Bergen, Norway
[2] Norwegian university of Science and Technology.

Abstract

Stiffened plates may be loaded by axial forces in two directions, i.e., along and transverse to the stiffeners, by in-plane shear force, and by out-of-plane loads as from traffic or water pressure. Special care must be taken for buckling effects caused by the compressive in-plane forces.

The buckling behaviour of plates stiffened with four trapezoidal stiffeners was investigated for the case of compressive axial force directed transverse to the stiffener direction. The width and length of the stiffened plate and the ratio between the plate- and stiffener stiffnesses were varied. The investigation aimed to determine criteria to ensure that the dominating buckling mode was either buckling of the plate between the stiffeners, or a predictable buckling pattern of the stiffeners. For this, two formulas are presented, giving the necessary plate-to-stiffener stiffness ratio or the maximum length of the panel. Furthermore, capacity approaches for the axial resistance for transverse axial loading are studied, applying the Effective Width Method (EWM) and the Reduced Stress Method (RSM). Comparisons with nonlinear FE-simulations show that the predictions range from 45% to 99% of the FE-results.

Keywords

Stiffened plate, axial force transversely to the stiffener, trapezoidal stiffener, elastic critical stress, Eurocode, buckling resistance.

1 Introduction

Stiffened plates are often used in structures that require high resistance and low weight. Examples include ship hulls, box girders and plate girders in bridges, offshore floor decks and module walls, etc. The primary function of the stiffeners is to stiffen the plate against buckling for in-plane compression forces or in-plane shear. For panels with axial compressive force in the same direction as the stiffeners, i.e., longitudinally stiffened plates, the stiffeners participate significantly in resisting the axial force. For axial force directed perpendicular to the stiffener direction, the plate carries the entire force, and the stiffeners are normally less effective in restraining the buckling. Panels with an axial force perpendicular to the stiffeners are referred to as "transversely stiffened panels (or plates)" in this paper. Figure 1 shows the loading case. The length of the panel is *e* (direction along the stiffeners), and *f* is the width of the panel.

The Effective Width Method in the structural Eurocodes only accounts for unstiffened plates and longitudinally stiffened plates. The Reduced Stress Method, however, also considers stiffened plates subjected to in-plane normal force directed transversely to the stiffeners, and combined load situations. The description of the RSM is improved in the second generation of the Eurocodes. An essential element in the strength calculation for a stiffened panel is the determination of the critical buckling stresses, which usually must be performed using FE tools.

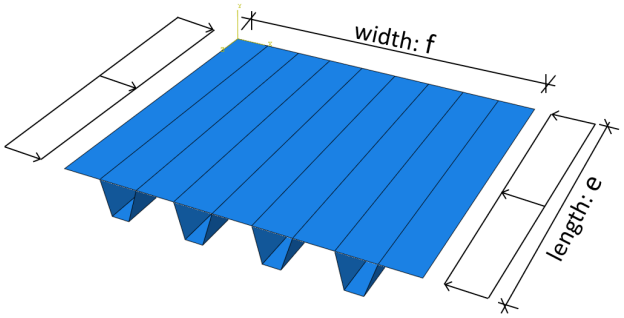

Figure 1 Plate stiffened with trapezoidal stiffeners, loaded transversely to the stiffeners.

https://doi.org/10.1002/cepa.2527 wileyonlinelibrary.com/journal/cepa

The first buckling mode (lowest buckling force) for a transversely stiffened panel is a buckling with one or more half-waves in the direction of the loading (*f*), with, in many cases, only one half-wave in the stiffener direction (*e*). The actual buckling shape depends on the panel's length-to-width ratio (*e*/*f*), the thickness of the plate, the spacing of the stiffeners, and the stiffeners' bending- and torsional stiffness. In contrast, for a plate loaded with axial force in the direction of the stiffeners, buckling may be several half-waves along the stiffeners. If the cross-section and panel dimensions of a transversely stiffened plate are such that the plate buckles in several half-waves in the direction transverse to the stiffeners, with zero out-of-plane displacements along the connections to the stiffeners, each stiffener will only affect one plate-buckle half-wave. Theoretically, if the stiffeners are placed in line with the natural zero-displacement lines in a buckled long plate, the bending stiffness of the stiffeners has no effect on the plate's elastic buckling resistance [1].

Loading cases comprising plate membrane stresses directed transversely to the stiffeners occur in ship hulls, deck structures, and bridge beams, particularly in connection with launching operations or at concentrated forces or support points. The most common is probably to have combinations of longitudinal and transverse axial force situations.

The literature on the design of transversely stiffened plates is scarce. The present Eurocode, EN 1993-1-5, gives no direct guidance for calculating the critical buckling stress or capacity for plates loaded with axial force transversely to the stiffeners. In the second generation of the Eurocodes, the Reduced Stress Method is improved and can be used for such problems.

This paper investigates the critical buckling behaviour and capacity for transverse axial loading, focusing on plates stiffened with trapezoidal (closed) section stiffeners. Compared to open stiffeners (flat, T and L), closed stiffeners increase the plate's buckling strength because of i) the much higher torsional rigidity of the closed stiffeners, ii) the rotational stiffening to the plate from the walls of the closed stiffeners.

2 Elastic critical buckling stress for transversely stiffened panel

As a starting point in finding a simplified resistance model for transversely stiffened panels, this paper investigates how the elastic buckling modes vary along with the stiffener size and the panel's length-to-width ratio. First, current analytical and numerical solutions for determining critical buckling stress are discussed.

2.1 Analytical solutions

In reference [2], Troitsky presented an energy approach solution, also solved by Timoshenko [3], for the critical buckling stress of a transversely stiffened plate. The plate has equidistant stiffeners of open cross-section, with assumed zero torsional stiffness. Referring to Figure *2*, the solution assumes buckling with several buckling half-waves (*m*) along the load direction (*a*) and one half-wave in the stiffener direction (*b*). The critical stress of the plate is given by:

$$\sigma_{cr} = \frac{\pi^2 D}{b^2 t} \cdot \frac{\left(m^2+\beta^2\right)^2 + r\gamma\beta^3}{\beta^2 m^2} \quad (1)$$

$$\text{with } D = \frac{E \cdot t^3}{12(1-\nu^2)},\ \beta = \frac{a}{b}\ \text{, and } \gamma = \frac{EI_i}{bD} \quad (2)$$

The factor *r* in (1) is the number of stiffeners + 1 (*r*=*i*+1), equal to the number of plate spans along the length *a*. Stiffness EI_i is the flexural stiffness of each stiffener with a participating width of the plate.

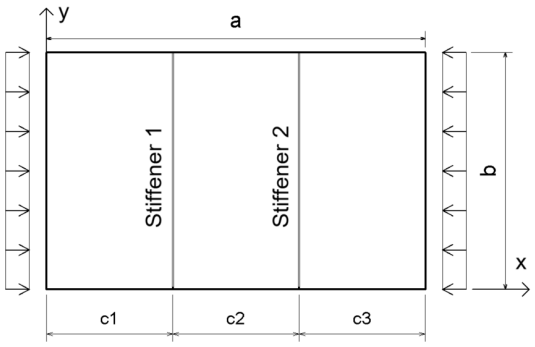

Figure 2 Axially loaded plate with equidistant transverse open section stiffeners, solution by [2, 3].

The above solution does not account for the significant torsional stiffness of closed-section stiffeners. Smith [4, 5] derived a solution for the same buckling problem. He included the torsional stiffness of the stiffeners in his research, which focused on fibreglass-reinforced plastic panels used in composite ship hulls. In reference [4], he presented the critical load for three buckling modes, reproduced in Figure 3.

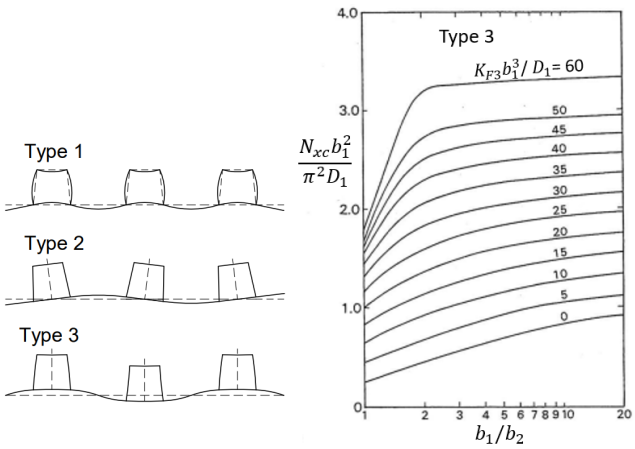

a) Buckling modes *b) Example for type 3 buckling*

Figure 3 Buckling types and diagram (Smith [4]).

Type 1 and Type 2 in Figure 3 are buckling modes with zero out-of-plane displacements of the stiffener but with stiffener wall bending and torsional rotation of the stiffeners, respectively. Type 3 is a systematic up-and-down buckling of the stiffeners. Smith divided the panel into rectangular plate strips representing the elements of the plate and the stiffeners and solved the critical buckling load by using a "folded-plate analysis" involving differential equations and work equations. The solutions were given by formulas and by diagrams [4], illustrated for the "Type 3" mode in Figure 3b. Especially in box- and plate girders in

bridges, as well as for some deck structures, closed stiffeners are preferred.

In [6], the present authors investigated the Troitsky/Timoshenko [2, 3] and Smith [4] buckling load solutions for stiffened aluminium panels with either open or trapezoidal stiffeners and compared them with shell element FE analyses (Abaqus). The predictions by the Timoshenko solution were found to be generally good for plates with open T-shaped stiffeners and relatively conservative for plates with closed trapezoidal stiffeners. The theoretical elastic buckling loads for these two cases were approximately 80% and 38% of the FE prediction, respectively. The considerable underestimation of the elastic buckling load for plates stiffened with closed stiffeners is due to the neglect of the stiffeners' torsional stiffness and the neglect of the flexural stiffness of the stiffener walls, which constrains the plate buckling. The Smith solution provided better critical load predictions, approximately 60% of the FE-prediction (a thorough discussion on this is given in [6]).

Recently, Williams et al. [7] reported an investigation on elastic buckling of offshore steel structures with plates loaded transversely to the stiffeners. Similarly, as Timoshenko [3], they developed analytical methods for finding the critical buckling load by applying differential equations and series summations.

2.2 Numerical solutions

One convenient way to determine elastic critical buckling load of stiffened rectangular plates is to apply the calculation program EBPlate [8], which considers the torsional rigidity of the stiffeners, as well as the local rotational stiffness provided to the plate from the webs of closed stiffeners. In [6], the authors showed that for plates stiffened with trapezoidal stiffeners, the transverse buckling load predictions by EBPlate agreed reasonably well with more advanced FE-shell element results (Abaqus). The EBPlate predictions were approximately 80 % of the FE-results. In most cases, simplified solutions are sufficiently accurate to be used to determine a stiffened plate's capacity.

3 Buckling modes for transversely stiffened panels

Elastic buckling analyses were carried out using FE shell models of transversely stiffened panels to find how different buckling modes vary with variations in the panel geometry. The stiffener size and the width/length ratio of the panels were changed systematically to detect the transition point between the three lowest buckling modes of the panels.

3.1 Overview of buckling shapes

For plates stiffened with trapezoidal stiffeners like in Figure 1 and panel length-to-width (*e/f*) ratios smaller than approx. 2, the buckling shapes are dominated by three modes. These modes are illustrated in Figure 4 for a panel with four trapezoidal stiffeners with equal *c/c* spacing (distance between the stiffeners centrelines). For the investigated range of geometries, it was found that with small lengths of the panel (*e*=small) relative to the bending stiffness (*EI*) of the stiffeners, the stiffeners were sufficiently rigid to remain straight so that the axially loaded plate buckled in a systematic up-and-down buckling both between the stiffeners and inside the stiffener cells. This buckling mode, a "plate-buckling", is shown in Figure 4a. The buckling mode in the figure contains nine half-wave buckles in the panel's width direction (*f*), i.e., transverse to the stiffeners. By increasing the length (*e*) of the panel, one reaches a panel length where the stiffeners buckle up or down, as illustrated in Figure 4b. Alternatively, the panel buckles with plate buckles, but with one or two less half-waves (Figure 4c). This latter Mode has seven or eight half-waves in the loaded direction (*f*) and some torsional rotation of the stiffeners. In the following, the perfect plate buckling mode is named Mode A, the up-and-down buckling of the stiffeners is named Mode B, and the buckling mode with one or two fewer half-waves than the perfect plate buckling mode is named Mode C. By further increasing the length e of the panel, all the stiffeners tend to buckle in the same direction in the lowest buckling mode with one or two buckling waves along the stiffeners in the stiffened plate. This paper focuses only on panels with lengths that give the lowest buckling mode A, B or C, which will be the case for common panel geometries.

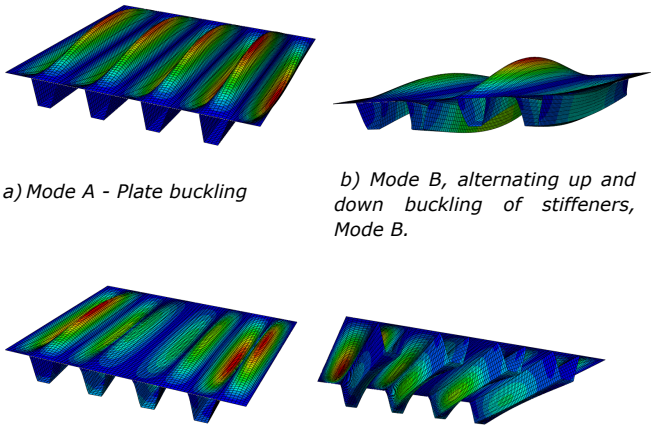

a) Mode A - Plate buckling

b) Mode B, alternating up and down buckling of stiffeners, Mode B.

c) Mode C - Plate buckling with one less half-wave in the width direction compared to Figure a, some distortion of the stiffeners.

Figure 4 Buckling modes, transversely stiffened plate.

The buckling analyses were designed to determine for which geometries the lowest eigenvalue (first buckling mode) of the stiffened panel changed from Mode A to Mode B or Mode C. The different modes were obtained by changing the panel length (*e)* while keeping the width (*f*) constant and varying the stiffeners' dimensions such that their torsional stiffness varied relative to their bending stiffness. For large torsional rotational stiffness (GI_t) to bending stiffness (*EI*) ratio for the stiffeners, the stiffeners remained without torsional rotation, and the first buckling mode changed from Mode A to Mode B at a certain length of the panel. The buckling mode shifted from Mode A to Mode C for torsionally softer stiffeners. The intention of the following is to explain when the transition from plate buckling to plate/stiffener buckling and twisting of the stiffener occurs and how this may be used in the dimensioning of a transversely stiffened panel.

3.2 FE-analyses and model

The following analyses were performed to determine the geometric parameters for when Mode A, B and C occur. The investigation focused on a panel with four equally spaced trapezoidal stiffeners. The loading was a uniformly distributed in-plane axial force transverse to the stiffeners (membrane force). The panel dimensions were chosen as shown in Figure 5. To obtain a buckling mode with local plate buckling (Mode A) with equal amplitudes for the nine half-waves along the width of the panel (Figure 4a), each sub-plate (i.e., plate part inside the stiffeners and plate part between the stiffeners and at the edges) were given equal widths ($2a_1$), as shown in Figure 5. In the analyses, the length (e) of the panel was varied to find the maximum length that yielded a buckling mode with pure plate buckling. At least two analyses were necessary for each panel geometry to determine this length. Similar results were also obtained with panels with 3, 5 and 6 stiffeners. The investigated geometries (96 models in total) are explained in Table 1.

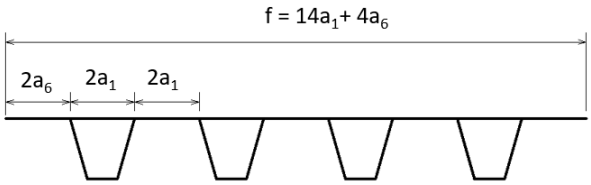

a) Cross section of the panel

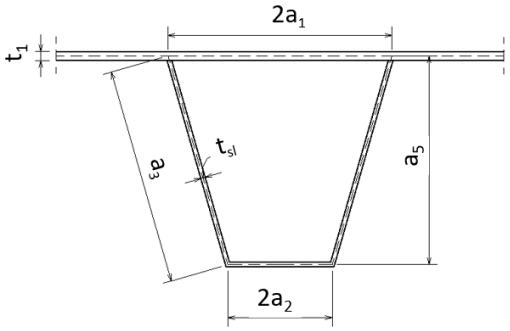

b) Cross-section of stiffener and belonging plate, the dimensions refer to the system lines. Symbols for dimensions conform to EN 1999-1-1.

Figure 5 Cross-section of panel with four stiffeners.

Table 1 Range of geometries.

$f/2a_1/2a_6$ [mm]	$2a_2$ [mm]	a_5 [mm]	t_1 [mm]	t_{sl} [mm]	n_{sim}	$\gamma = \frac{I_{sl}}{I_p}$
2160/ 240/240	120, 150	170, 240	12,16, 20, 24	6, 10, 16, 20	64	59-1905
2700/ 300/300	140, 180	210, 280	12,16, 20, 24	6, 10, 16, 20	64	87-2486
3600/ 400/400	200, 300	320, 400	12,16, 20, 24	6, 10, 16, 20	64	199-5288

I_{sl} = the second moment of area of the whole stiffened plate

$I_p = \frac{f \cdot {t_1}^3}{12(1-\nu^2)}$ = second moment of area of the plate only

As seen from Table 1, the width of the panel was varied from 2160 mm to 3600 mm, such that the width of the subpanels of the plate (inside stiffeners, between stiffeners/at the edges, $2a_1$ and $2a_6$, respectively) was varied from 120 mm to 400 mm. Four plate thicknesses were used, 12 mm, 16 mm, 20 mm and 24 mm. The width of the stiffener flange ($2a_2$) was varied from 120 mm to 300 mm, while the height of the stiffener (a_5) was varied from 170 mm to 400 mm, keeping an almost constant stiffener web angle. The stiffener plate thicknesses were 6 mm, 10 mm, 16 mm and 20 mm. Classification of the sub-plate elements of the plate and stiffeners according to regular cross-section classes has no direct relevance as the loading is directed transversely to the stiffener direction.

The panels were modelled in the FE program Abaqus [9], with a model as shown in Figure 6. Four-node linear shell elements were used, with an element size of approximately 30x30mm. At least four elements were used over the width of the stiffener walls and the width of the plate inside- and between the stiffeners. This provided sufficiently fine-meshed models to determine the buckling shapes and loads of the panel. All four edges of the plate and the end section of the stiffeners were supported in the z-direction. In-plane compressive displacement loading (x-direction) was applied on Edge B, while the x-displacement was restrained at the opposite side (Edge A).

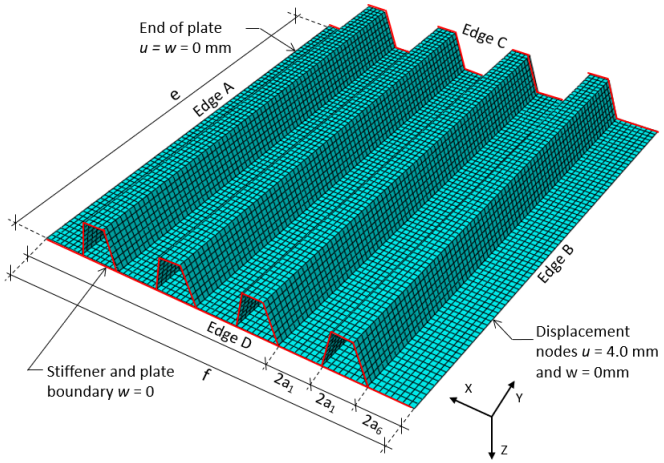

Figure 6 Shell element model of the panel with four stiffeners.

The initial idea of the study was to seek the maximum length of the panel, which maintained local plate buckling as the lowest eigenvalue, i.e., with the stiffeners remaining straight. By viewing the various shapes, it was seen that plate buckling, in many cases, was accompanied by stiffener wall deformations. This occurred even for relatively short panel lengths (e). The buckling shape was also sensitive to the width ($2a_6$) of the subpanels at the side of Edges A and B (Figure 6). To maintain a "repeated geometry", these side-panels were modelled with a width equal to the width of the plate sub-panels between the stiffeners and inside the stiffeners, i.e., with a width $2a_6$=$2a_1$. However, as Edge A and B of the stiffened panel were simply supported, the side-panels had a rotational freedom not present for the interior subpanels of the plate, which were rotationally restrained by their connection to each other and to the webs of the stiffeners. For the present case, with an axial force directed transversely to the stiffeners,

this difference caused the buckling to be dominated by the weaker side-panels. Therefore, to simplify the problem, a hinged connection was introduced between the main plate and the webs of the stiffeners along all eight junction lines. The effect of this simplification on the elastic critical buckling stress and resistance of the panel is exemplified in the following.

3.3 Buckling Mode A

As noted in Section 3.1, the local plate buckling, Mode A with nine plate half-waves, appears as the first buckling mode for relatively short panels. By increasing the length (e), the first buckling mode either changes to Mode B, stiffener buckling with four half-waves where the stiffeners are displaced in alternating directions, or to Mode C with eight or seven half-waves in the plate with some rotation/distortion of the stiffeners. Panels that buckle in Mode C as the first buckling mode change to Mode B when the panel length is increased sufficiently.

Based on the buckling analysis results, using some trial and error and curve fitting, two transition limits were established. Equation (3) is for the transition from Mode A to B, while Equation (4) is for the transition from Mode A to C.

$$\frac{EI^*_{sl,i}\cdot(2a_1)^2}{e^3 D} < \beta \qquad (3)$$

$$\frac{2a_1\cdot {t_1}^2\cdot e}{I^*_{sl,i}} > \theta \qquad (4)$$

The transition limits are the factors β and θ. $I^*_{sl,i}$ is the second moment of area of one trapezoidal stiffener, including a $10t_1$ width of the plate to each side of the stiffener webs. E is the elastic modulus, and D is the plate stiffness: $D = \frac{E\cdot t_1^3}{12(1-\nu^2)}$. From the two formulas, one may either determine a maximum length of the panel, $e = e_{max}$, which holds local plate buckling as the first buckling mode, or one may determine a necessary second moment of area of the stiffener ($I^*_{sl,i}$) to maintain such buckling. As an example, Table 2 gives the data for a 16 mm thick plate (t_1= 16mm) with the varied stiffener geometry (widths and thickness). The table gives the panel length (e_{max}) found in Abaqus for the transitions between Mode A to B or Mode A to C, and the elastic buckling stress of the panel (σ_{cr}) and the parameters β and θ for each of the investigated geometries. As shown, increasing the stiffener size leads to an increased e_{max}, i.e., the panel can be longer before the buckling of the stiffeners becomes critical. The critical buckling stress is relatively constant for a given sub-panel width ($2a_1$), which agrees with a typical plate-buckling mode in the sub-panels (Figure 4a). The numerical buckling stress σ_{cr} also fits very well with the analytical solution of a subpanel with length e and width $2a_1$.

Table 2 Results for panel with 16 mm plate thickness.

$2a_1$	$2a_2$	a_5	t_{sl}	e_{max}	γ	σ_{cr}	eq. (3) β	eq. (4) θ
240	150	170	6	900	201	993	7,62	**1,53**
	150	170	10	1150	296	940	5,38	**1,33**
	150	170	16	1600	410	910	**2,77**	1,33
	150	170	20	1700	475	904	**2,67**	1,22
	120	240	6	1100	411	949	8,54	**0,91**
	120	240	10	1500	600	913	4,92	**0,85**
	120	240	16	2000	829	894	**2,86**	0,82
	120	240	20	2100	960	893	**2,87**	0,75
300	210	210	6	1300	300	606	7,36	**1,48**
	210	210	10	1800	442	580	4,09	**1,39**
	210	210	16	2300	613	568	**2,72**	1,28
	210	210	20	2400	710	565	**2,78**	1,15
	140	280	6	1600	532	586	7,01	**1,03**
	140	280	10	2300	780	568	3,46	**1,01**
	140	280	16	2700	1080	563	**2,96**	0,85
	140	280	20	2800	1252	560	**3,08**	0,76
400	210	320	6	2300	652	332	6,86	**1,20**
	210	320	10	3400	946	322	**3,08**	1,23
	210	320	16	3900	1299	321	**2,80**	1,02
	210	320	20	4100	1501	320	**2,79**	0,93
	200	400	6	2600	1081	325	7,87	**0,82**
	200	400	10	3900	1557	316	3,36	**0,85**
	200	400	16	4500	2131	314	**2,99**	0,72
	200	400	20	4700	2463	320	**3,04**	0,65

a_1, a_2, a_5 and t_{sl} in mm. Critical load stress σ_{cr} in N/mm². γ is defined in Table 1.

With the 24 combinations in Table 2 and the four plate thicknesses studied, the total number of geometry combinations was 96. As several lengths of each panel geometry had to be modelled to determine the different buckling modes and the transitions between modes, around 500 buckling analyses had to be run. The main outcome of each analysis was the transition length. The numbers in bold font in Table 2 show the values of factors β and θ that corresponds to the shortest panel length for the transition from Mode A to B or to C, respectively. Conservative values for the transition factors, to ensure that the plate-buckling (Mode A) is the first buckling mode, are β=3,2 and θ=0,82. Applying these values as constants in Equations (3) and (4) gives a requirement for the stiffener's second moment of area

$$I^*_{sl,i} > max\left[\left(\frac{3{,}2\cdot e^3\cdot D}{E\cdot(2a_1)^2}\right), (1{,}2\cdot 2a_1\cdot e\cdot {t_1}^2)\right] \qquad (5)$$

or a maximum length of the panel to maintain plate buckling.

$$e_{max} < min\left(\sqrt[3]{\frac{I^*_{sl,i}E\,(2a_1)^2}{3{,}2D}}, \frac{I^*_{sl,i}}{1{,}2\cdot 2a_1\cdot {t_1}^2}\right) \qquad (6)$$

Figure 7 shows a plot of the data points of Table 2 (and the required second moment of area $I^*_{sl,i}$ from Equation (5). The data points from the analyses for each of the varied sub-plate widths and stiffener-height combinations ($2a_1/a_5$) are connected by broken lines. The continuous

lines are the requirements of Equation (5). As shown, all FE results are either on the safe side of Equation (5) or on the curves. For some geometries, the required $I^*_{sl,i}$ is significantly on the safe side, at the most 1,53/0,82 = 1,9 times the one determined in the FE analysis (found from θ in eq. (4), right column in Table 2) . The most conservative results appear for panels with a stiffening ratio below approximately γ = 600 (this ratio is defined in Table 1).

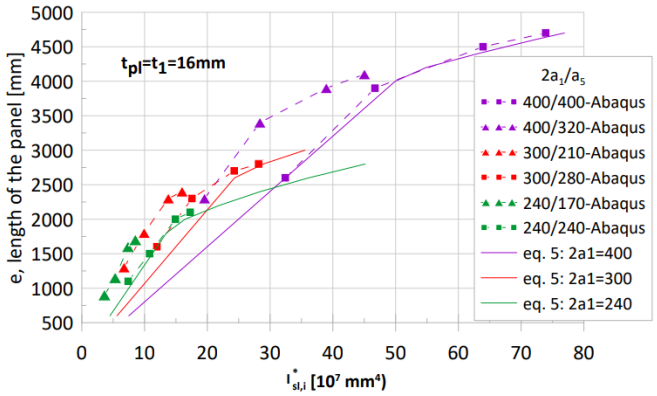

Figure 7 FE-results and Equation (5) for plate thickness t_1=16mm.

Similar comparisons are made for panels with plate thicknesses t_1 = 12, 20 and 24 mm in Figure 8 to Figure 10. As seen, all the FE-results are on the safe side. If the comparisons were limited to plates with stiffener sections of "equal" width and height, $2a_1 \approx a_5$, the required values of $I^*_{sl,i}$ from Equation (5) agrees in general very good with the FE-results, with less than 45 % deviation.

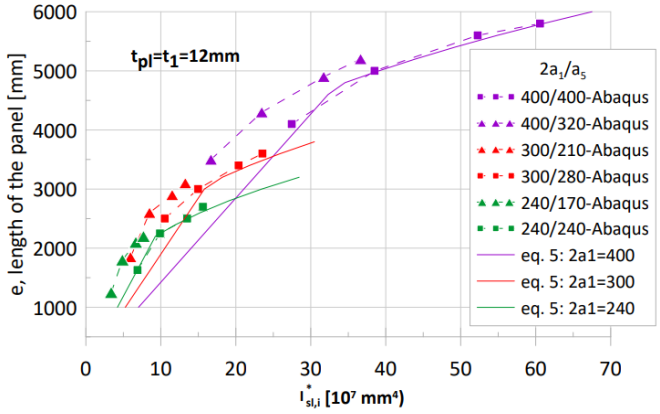

Figure 8 FE-results and Equation (5) for plate thickness t_1=12mm.

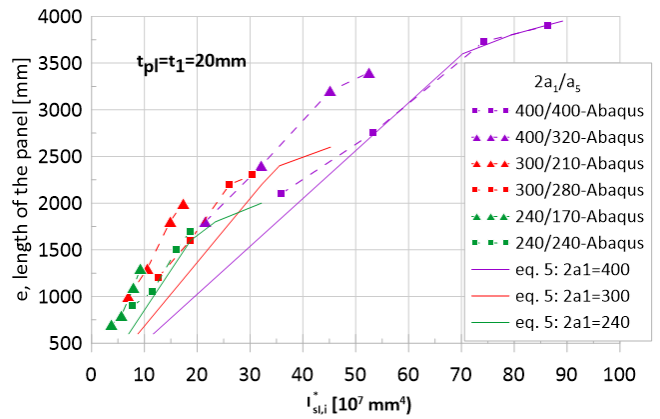

Figure 9 FE-results and equation (5) for plate thickness t_1=20mm.

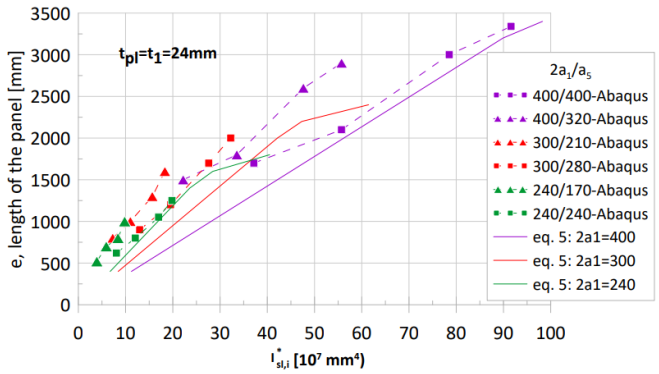

Figure 10 FE-results and Equation (5) for plate thickness t_1=24mm.

3.4 Buckling Mode B

As discussed in Section 3.1, the first elastic buckling mode is Mode A for short panels and Mode B for medium-long panels up to some limit. Mode A is the easiest buckling shape to consider in the design, as the plate remains straight along the stiffener webs, and the design may be done by considering a sub-plate or a plate strip across the stiffened panel, with support at the stiffeners. For Mode B, with the alternating up-and-down buckling of the stiffeners (four half-waves across the stiffened panel), another strip model may be established – having an adequate buckling length. It is thus interesting to also establish an estimate for the panel length (a length range) where Mode B appears as is the first buckling mode for the stiffened panel.

With the geometries of Table 1 and analysis results from the 96 different panel geometries in longer lengths, a limit for the second moment of area of the stiffener that ensures Mode B may be suggested:

$$I^*_{sl,i} \cdot (2a_1)^2 > \frac{0{,}45 \cdot e^3 \cdot D}{E} \qquad (7)$$

The equation is similar to Equation (3), here with the β factor of 0,45. Figure 11 shows the curves for the equation together with the FE results for the four plate thicknesses, all presented in one diagram made possible by incorporating the geometrical dimension $2a_1$ into the horizontal axis. The diagram shows the maximum length of the panels to ensure buckling by stiffener displacements, or it may be used to determine the upper value for the second moment of area of the stiffener. The suggested criterion Equation (7) fits quite good with the FE analysis results, with the largest deviations for 16 mm and 20 mm plate thicknesses.

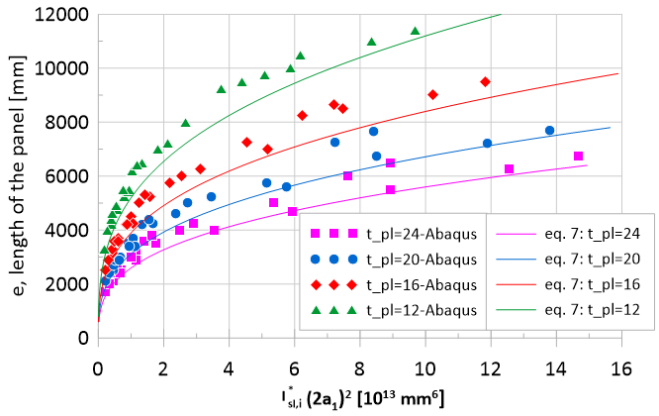

Figure 11 Mode B, FE-results and Equation (7).

4 Capacity for transverse axial loading

Two sets of design approaches are outlined in the following, one for the stiffened panel when it buckles according to Mode A with the systematic buckling of the plate only, and another for when it buckles in Mode B with the alternating up and down deflections of the stiffeners. The simple design approaches may be used for the estimation of plate and stiffener dimensions/spacing for a given case. Still, they cannot capture the interaction between buckling forms or cases where the inelastic buckling pattern is very different from the elastic modes.

4.1 Design for Mode A - plate buckling

In Mode A the plate buckles as shown in Figure 4a with one buckle in each sub-panel between the support lines along the connection to the stiffeners. The long dimension of the buckle is oriented parallel to the stiffeners, and the short direction is transverse to the stiffeners. In Mode B (Figure 4b), both the plate and the stiffeners deflect, and the transverse buckles in the plate become longer (and fewer).

As an example, Example 1, a stiffened panel with four stiffeners is assumed. The panel width (f) is 2700 mm, and the other dimensions a_1=a_6=150, a_5=280, t_1=12 and t_{sl}=10 (all in mm). The stiffeners have a second moment of area $I^*_{sl,i}$ = 1,498· 10^8 mm^4. Applying Equation (6), the panel's maximum length (e) to maintain buckling Mode A becomes 2880 mm, which is used for the length in the following. For determining the panel's resistance to transverse axial force, three methods are applied, i) the effective width method given in FprEN 1993-1-5: Plated structural elements [10] (with the renewed interpolation function between plate buckling and column buckling behaviour), ii) the reduced stress method of FprEN 1993-1-5 where the critical stresses for plate- and column buckling of the stiffened panel are needed as input in the calculation, and iii) a geometrically and materially nonlinear FE-analysis in Abaqus like the model in Figure 6.

The modelled material is S355 with yield stress 355 N/mm² with a strain hardening E/10000 as prescribed in prEN 1993-1-14 Design assisted by finite analysis [11]. Imperfections and residual stresses due to fabrication are included by an equivalent imperfection according to clause 5.4.4 of [11]. The prescribed magnitude of the imperfections of the sub-panels of the plate is min(a/200, b/200), which corresponds to 300mm/200=1,5 mm in the example. The required bow imperfection for a welded stiffener is the stiffener length divided by 400, i.e., 2880mm/400=7,2 mm. However, an imperfection of this size for the systematic up-and-down initial deflection of the stiffeners seemed unrealistic, so half of this was used, i.e., 3,6 mm. The imperfections were imposed in the FE model by importing scaled fractions of the elastic buckling modes A and B. The FE model was loaded by an incremental compressive displacement of Edge B to a displacement of 4,0 mm (Figure 6).

Furthermore, imperfections were modelled according to [11], applying a leading imperfection combined with 70% of an accompanying imperfection, where each imperfection was tested as the leading. As buckling mode B also contains significant deflections of the plate, the amplitude of this imperfection was reduced when combined with Mode A (see Table 3 for combinations).

Table 3 shows the determined elastic buckling stresses for the stiffened panel, and the results of the three methods i), ii) and iii) with the buckling reduction factors and the ultimate axial force resistances (without material factors). Results for three versions (version A, B and C) of the panel are given.

Table 3 Results for stiffened panel with length e=2880 mm and width f=2700 mm, Example 1.

Version A - with a hinged connection between the plate and stiffener webs	
Critical buckling stress obtained by Abaqus: Plate behaviour: $\sigma_{cr.pl}$ =316 N/mm² Column behaviour: $\sigma_{cr.c}$ =308 N/mm²	Resistance $N_{b.Rd}$
i) Effective width method for sub-panel, 2880 mm wide and 300 mm long, assumed simply supported on all four edges: Buckling reduction factor ρ=0,547.	6710 *kN*
ii) Reduced stress method, which considers the entire panel: Reduction factor ρ=0,560.	6870 *kN*
iii) Abaqus nonlinear capacity analysis, applying imperfection 1,5 mm of Mode A and 1,1 mm of Mode B. Capacity is taken as the ultimate force from the nonlinear response curve.	7040 *kN*
Version B - a rigid connection between the plate and webs of stiffeners	
Critical buckling stress obtained by Abaqus: $\sigma_{cr.pl}$ = 405 N/mm², $\sigma_{cr.c}$ = 399 *N/mm²*	
i) Effective width method for sub-panel as above:	6710 *kN*
Using a column-buckling approach for the capacity of the plate, with a plate strip with a buckling length of 0,86·300=258 mm: Column buckling reduction factor ρ=0,642.	7880 *kN*
ii) Reduced stress method, which considers the entire panel: Reduction factor ρ=0,638.	7840 *kN*
iii) Abaqus nonlinear capacity analysis, applying an imperfection 1,5 mm of Mode A and 1,1 mm of Mode B	7890 *kN*
Version C - longitudinal slit in the flange of stiffeners, rigid connection between plate and webs of stiff.	
Critical buckling obtained by Abaqus: $\sigma_{cr.pl}$ = 293 N/mm², $\sigma_{cr.c}$ = 287 *N/mm2*	
i) Effective width method for a typical sub-panel not relevant	-
ii) Reduced stress method, which considers the entire panel: Reduction factor ρ=0,535.	6570 *kN*
iii) Abaqus nonlinear capacity analysis, applying imperfection 3,6 mm of Mode B.	7210 *kN*
Calculations apply buckling curve α=0,34	

First, the panel was modelled with a flexural hinged connection between the plate and the webs of the stiffeners (as modelled in Section 3). This version is identified as "Version A" in Table 3. Then the panel was modelled with the plate and the stiffener webs rigidly connected as would be the normal outcome of welded stiffeners ("Version B"). Lastly, to also cover the case of plate stiffened with open-section stiffeners, a model where a longitudinal slit was modelled in the bottom of each of the trapezoidal stiffeners (which transforms each closed stiffener into two L-shaped stiffeners) was investigated ("Version C"). For the RSM, the critical plate buckling stress was determined from the FE-model in Figure 6, while the critical column buckling stress was extracted from a similar model but without out-of-plane support (z-direction) at plate Edges C and D (Figure 6), as prescribed in FprEN 1993-1-5 clause 12.4(8) [10].

As shown in Table 3 for Version A, the effective width method applied on the assumed simply supported 2880 mm wide and 300 mm long subpanels of the main plate gives an axial force resistance ($N_{b,Rd}$) of 6710 kN. The compressed cross-sectional area of the plate is $b \cdot t$=2880·12 mm^2. For Version B, with the rigid connection between the plate and the webs of the stiffeners, a column strip model which accounts for the elastic restraints from the stiffener walls (determined in a frame model analysis) gives an effective buckling length of 0,86 ·300mm =258 mm for the strip, which gives a resistance of 7880 kN for the 2880 mm wide plate column. The reduced stress method gives resistance of 6870 kN for Version A and 7840 kN for Version B. The difference is mainly caused by the differences in the stiffened panel's critical stresses (for plate and column behaviour).

If the axial resistances determined by Abaqus are used as references, i.e., 7040 kN for Version A (hinged connection of the stiffener webs) and 7890 kN for Version B (rigid connection), it may be concluded that the modelling of the stiffener web-to-plate junctions as flexural hinged connections (Version A) yields conservative, but acceptable results for the axial capacity of the transversely stiffened panel. The effective width approach considering only a sub-panel of the main plate gives quite good results, with predictions 6710kN/7040kN = 0,95 and 6710kN/7890kN = 0,85 times the Abaqus resistances, for Version A and B, respectively. The column strip model accounting for the rigid connection between the plate and the stiffener webs gives resistance 7880kN/7890kN = 0,999 of the Abaqus prediction, i.e., very accurate in this case. The resistances obtained with the reduced stress method are also very accurate for both versions, with resistances 0,98 and 0,99 times the Abaqus predictions, respectively.

For the model Version C, with the four trapezoidal stiffeners converted into eight L-shaped stiffeners, the resistance obtained by Abaqus is 7210 kN, which is significantly less than for Version B (7890 kN). The difference is likely due to the combination of less flexural rigidity of the stiffener webs and less torsional rigidity of the open-section stiffeners. With the eight open L-stiffeners, the lowest elastic buckling mode of the plate is no longer a buckling with nine half-waves. Therefore, the effective width buckling model for the sub-panels between stiffeners cannot be applied. The resistance may, however, still be accessed by applying the reduced stress method (using the plate- and column critical stresses from Abaqus for this geometry), and gives, in this case, an axial resistance of 6570 kN, which is 91 % of the ultimate resistance predicted by the nonlinear simulation in Abaqus.

Other panels with the same stiffener geometries and length as above, but with 3, 5 and 6 stiffeners, were also analysed with Abaqus (with the hinged connection between the plate and the stiffener webs). The results for the elastic buckling stresses and axial load resistances for transverse compression were almost identical to the corresponding results in Table 3. This indicates that a general design model based on buckling of a sub-panel of the main plate (as in Table 3) may be applicable for a larger range of panel widths (and numbers of stiffeners), provided that the requirement of either Equation (5) or (6) which ensures buckling Mode A is fulfilled.

4.2 Design for Mode B – stiffener buckling

For buckling Mode B, where every other stiffener buckle either up or down, there is obviously a strong interaction between the stiffener- and plate deflections. The elastic buckling shape is shown in Figure 12, where Figure b shows a cross-section at the midspan (displacements from Abaqus). In the interior of the stiffened panel the distance between the inflexion lines of the buckled plate is typically $4a_1$, as indicated in the figure. In the regions at the side edges of the panel the distance between the inflection lines is somewhat larger, approximately $2a_6 + 3a_1$. The difference is connected to the actual width ($2a_6$) of the subplate outside the outermost stiffener at each side and the rotationally hinged support along the long exterior edge of the plates.

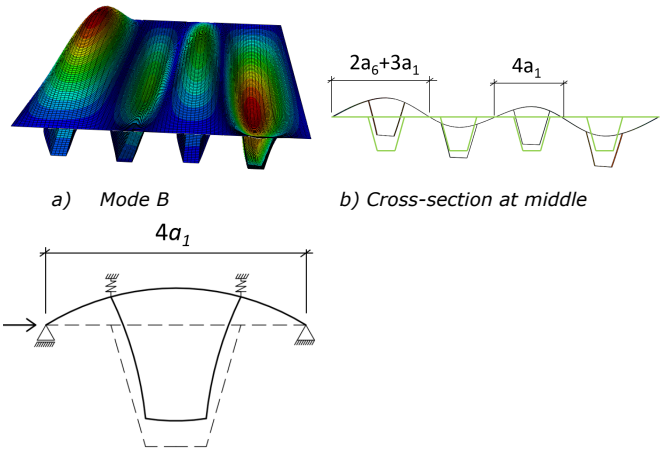

Figure 12 Buckling of the stiffened panel, Mode B, and deflection shape.

A simple resistance model for this Mode B buckling may be established by considering a typical transverse strip of the stiffened panel, across one interior stiffener, as shown with the model in Figure 12c. The axial loading is the membrane force transverse to the stiffeners. The considered width is $4a_1$, corresponding to the width of the stiffener cell plus the belonging part of the plate at each side. If the plate strip across the stiffener is considered as an isolated column, it has buckling curvature only in the direction transverse to the stiffener. The effective buckling length

for this column may be estimated by various methods, e.g., a frame type of analysis or a beam on an elastic foundation. The restraints to the buckling of the column are the longitudinal flexural stiffness of the stiffener and the transverse flexural stiffness provided by the plates of the stiffener, as indicated in Figure 12c. The buckling length for the plate strip may also be determined from the elastic critical buckling load of the panel (Figure 12a) determined by the FE analysis, which in this case gives buckling lengths $0{,}84 \cdot 4a_1$ and $0{,}59 \cdot 4a_1$ for modelling Version A and B, respectively.

Example 2 is based on a panel with four stiffeners and a cross-sectional geometry identical to that of Example 1 in the previous. The length of the panel is now taken as the maximum length ($e=e_{max}$) of the panel, which holds buckling Mode B as the first buckling mode. The length is determined using Equation (7), which gives:

$$e_{max} = \sqrt[3]{\frac{I^*_{sl,i} E\,(2a_1)^2}{0{,}45D}} = 5740mm \qquad (8)$$

As mentioned in section 3.1, by increasing the length e of the panel past 5740 mm (the maximum length holding first buckling mode B), all stiffeners tend to buckle in one direction, causing an overall buckle.

The calculations and FE results are given in Table 4. As for Example 1, three methods for determining the transverse axial resistance of the stiffened panel are studied: the effective width method, the reduced stress method, and the nonlinear simulation in Abaqus. Table 4 shows a significant spread in the predicted axial force capacities (from 2150 kN to 9410 kN). For this example, there is no difference in the FE elastic critical stress predictions between the plate- and column case. The attempt (i) to apply the effective width method for the 5740 mm wide and 600 mm long sub-plate element gives very conservative results, with a predicted axial resistance of approximately 25 % of the resistance determined by the nonlinear Abaqus analysis. As the stiffening effect from the stiffener is not accounted for in the EWM model, such conservative results could be expected. The column strip approach, which considers the reduced buckling length of the plate due to the buckling restraints provided by the stiffener, gives a somewhat better result. The predicted axial force resistance is for Version A (hinged connection between plate and stiffener webs) 2910 kN, which is 34 % of the Abaqus resistance. For Version B (rigid connection), the predicted resistance is 4210 kN, which is 45 % of the Abaqus result. The predictions by the reduced stress method (ii), which uses the plate- and column elastic critical stresses obtained with Abaqus, provide predictions (5470 kN and 7070 kN) that are 65 % and 75 % of the Abaqus resistances. The difference in the predicted resistances by Abaqus between versions A and B of the panel, i.e., flexural hinged versus rigid connection between the plate and the webs of the stiffeners, is approximately 10 %.

Table 4 Results for stiffened panel with length e=5740 mm and width f=2700 mm, Example 2.

Version A - with a hinged connection between the plate and stiffener webs	
Critical buckling stress obtained by Abaqus: $\sigma_{cr.pl}$ = 95,5 N/mm², $\sigma_{cr.c}$ = 95,5 N/mm².	Resistance $N_{b.Rd}$
i) Effective width method for sub-panel, the panel is 5740 mm wide and $4a_1$=600 mm long, and is assumed simply supported on all edges: Buckling reduction factor ρ=0,086.	2150 *kN*
Using a column-buckling approach for the plate strip across one stiffener (Figure 12c), with buckling length 0,84·600=506 mm: Buckling reduction factor χ_c =0,119	2910 *kN*
ii) Reduced stress method, which considers the entire panel: Reduction factor ρ=0,224.	5470 *kN*
iii) Abaqus nonlinear capacity analysis, applying an imperfection of 0,5 mm of Mode A and 3,6 mm of Mode B	8540 *kN*
Version B - rigid connection between the plate and webs of stiffeners	
Critical buckling stress from Abaqus: $\sigma_{cr.pl}$ = 128,6 N/mm², $\sigma_{cr.c}$ = 128,4 N/mm²	
i) Effective width method for sub-panel as above:	2150 *kN*
Using a column-buckling approach for the plate strip across one stiffener (Figure 12c), with buckling length of 0,59·600=416 mm: Buckling reduction factor χ_c =0,171	4210 *kN*
ii) Reduced stress method which considers the entire panel: Reduction factor ρ=0,289.	7070 *kN*
iii) Abaqus nonlinear capacity analysis, applying an imperfection 1,5 mm of Mode A	9410 *kN*

5 Summary

Design methods for stiffened plates loaded with in-plane compression directed transversely to the stiffeners' orientation are not well covered in the current steel Eurocode (EN 1993-1-1 and EN 1993-1-5). The new version, FprEN 1993-1-5, has a more detailed description of how to use the Reduced Stress Method (RSM) to calculate the design resistance for such panels. However, the RSM needs critical stresses from both column- and plate behaviour as input, which must often be calculated with FE simulations. Compared with open stiffeners, closed trapezoidal stiffeners have the advantage of high torsional rigidity and rotational stiffness in the junctions between the stiffeners and the plate.

This paper investigated the elastic buckling modes for transversely loaded panels with trapezoidal stiffeners, for plate- and stiffener geometry combinations where the governing buckling mode was either buckling of the plate only, or plate buckling with deflections of the stiffeners. To determine the likely elastic buckling mode of a stiffened panel, three equations were developed, based on a series

of FE shell element analyses in Abaqus. The primary parameters for determining the buckling modes and transition between modes are the second moment of area of the stiffeners ($I^*_{sl,i}$) and the length of the panel (e).

Furthermore, the paper investigated simplified methods to determine the resistance of the stiffened panel to transverse axial load. Having determined the elastic buckling mode of the panel, with either plate buckling or stiffener buckling as the first buckling mode, simplified plate (EWM) and column strip models were demonstrated to provide conservative estimates for the panel resistance. Here the ultimate resistances from Abaqus capacity simulations were taken as a reference. The simplified design models may be useful for a pre-study to select the geometry for the stiffened panel, whereas the final resistance verification should be done with nonlinear FE simulations.

Moreover, the reduced stress method of FprEN 1993-1-5, where the critical stresses for the stiffened panel's plate- and column buckling are needed as input, was shown to give quite accurate capacity predictions.

References

[1] Larsen, P. K. (2020) *Dimensjonering av stålkonstruksjoner.* 3. edition. Bergen: Fagbokforlaget.

[2] Troitsky, M.S.; Hoppmann, W. (1976) *Stiffened plates: Bending, stability, and vibrations.* Amsterdam – Oxford – New York: Elsevier.

[3] Timoshenko SP.; Gere JM. (1961) *Theory of elastic stability*. New York: McGraw-Hill.

[4] Smith CS. (1985) *Compressive strength of transversely stiffened FRP panels*. Aspects of the analysis of plate structures. 1985:149-74.

[5] Smith, C.S. (1972) *Buckling Problems in the Design of Fiberglass-Reinforced Plastic Ships*. Journal of Ship Research. 16 (1972) 174–190. https://doi.org/10.5957/jsr.1972.16.3.174.

[6] Kleppe, S-R.; Aalberg, A.; Langseth, M.; Fyllingen, Ø. (2023) *Buckling strength of a transversely stiffened aluminium deck.* Submitted for possible journal publication.

[7] Williams, D.M.; Eng, M.; Eng. P.; Sandwell, S.W. (2021) *Buckling of Transversely Stiffened Plates in Offshore Gravity-Based Steel Structures*. (12) (PDF) Buckling of Transversely Stiffened Plates in Offshore Gravity-Based Steel Structures (researchgate.net)

[8] EBPlate, v2.01 (2013) CTICM, France.

[9] Abaqus v6.22 (2019), Johnston, RI, USA.

[10] FprEN 1993-1-5: (as submitted to Formal Vote December 2022) Eurocode 3: (2023) *Design of steel structures, Part 1-5: Plated structural elements*. CEN.

[11] prEN 1993-1-14: (draft version September 2022): Eurocode 3: *Design of steel structures, Part 1-14: Design assisted by finite element analysis.* CEN.